Electronic Supplementary Information

pH-Responsive Supramolecular Vesicles Assembled by Water-Soluble Pillar[5]arene and BODIPY Photosensitizer for Chemo-Photodynamic Dual Therapy

Lu-Bo Meng,[a] Wenyi Zhang,[b] Dongqi Li,[a] Yan Li,[b] Xiao-Yu Hu,*[a] Leyong Wang,*[a] and Guigen Li [c,d]

[a] *Key Laboratory of Mesoscopic Chemistry of MOE and Collaborative Innovation Center of Chemistry for Life Sciences, School of Chemistry and Chemical Engineering, Nanjing University, Nanjing 210093, China. E-mail: lywang@nju.edu.cn, huxy@nju.edu.cn; Fax: + 86-25-83597090; Tel: + 86-25-83592529.*

[b] *State Key Laboratory of Bioelectronics, Jiangsu Key Laboratory of Biomaterials and Devices, School of Biological Science and Medical Engineering, Southeast University, Nanjing 210096, China.*

[c] *Institute of Chemistry and BioMedical Sciences, School of Chemistry and Chemical Engineering, Nanjing University, Nanjing 210023, China.*

[d] *Department of Chemistry & Biochemistry, Texas Tech University, Lubbock, Texas 79409-1061, USA.*

Table of Contents

1. Materials and Methods

All reactions were performed in atmosphere unless otherwise stated. The commercially available reagents and solvents were either employed as purchased or dried according to procedures described in the literature. Column chromatography was performed with silica gel (200-300 mesh) produced by Qingdao Marine Chemical Factory, Qingdao (China). All yields were given as isolated yields. Melting points (M.p.) were determined using a Focus X-4 apparatus (made in China) and were not corrected. NMR spectra were recorded on a Bruker DPX 300 MHz or 400 MHz spectrometer with internal standard tetramethylsilane (TMS) and solvent signals as internal references, and the chemical shifts (δ) were expressed in ppm and J values were given in Hz. 2D ROESY experiments were performed on a Bruker DPX 400 MHz spectrometer. Low-resolution electrospray ionization mass spectra (LR-ESI-MS) were obtained on Finnigan MatTSQ 7000 instruments. High-resolution electrospray ionization mass spectra (HR-ESI-MS) were recorded on an Agilent 6540Q-TOF LCMS equipped with an electrospray ionization (ESI) probe operating in positive-ion mode with direct infusion.

DOX Loading and Release of WP5⊃G Vesicles. DOX-loaded vesicles were prepared as follows: A certain amount of DOX was added to an aqueous solution of **G** (2% EtOH and 2% DMSO was added to improve the solubility of **G**), then a certain amount of **WP5** solution was added quickly, and finally water was added until the volume of the solution reached 10 mL. The ultimate concentrations of DOX, **G**, and **WP5** were 0.01, 0.05, and 0.025 mM, respectively. After standing overnight, the prepared DOX-loaded vesicles were purified by dialysis (molecular weight cutoff 10000) in distilled water for several times until the water outside the dialysis tube exhibited negligible DOX fluorescence. The DOX encapsulation efficiency was calculated by the following equation:

encapsulation efficiency (%) = $(m_{DOX\text{-}loaded}/m_{DOX}) \times 100$

where $m_{DOX\text{-}loaded}$ and m_{DOX} are mass of DOX encapsulated in vesicles and mass of DOX added, respectively. The mass of DOX was measured by the fluorescence

emission intensity at 550 nm and calculated as relative to a standard calibration curve in the concentrations from 0.69×10^{-7} to 34.11×10^{-7} M in water.

0.1 M tris-HCl (pH = 7.4) and 0.1 M citrate (pH = 6.0, 5.1, 3.9) buffer solutions were used as drug release media to simulate normal physiological conditions and the intracellular conditions of tumor. In a typical release experiment, 6 mL of DOX-loaded vesicles were added into 4 mL of appropriate release medium at 37 ^{o}C. At selected time intervals, 2 mL of the release media was taken out for measuring the released DOX concentrations by the fluorescence emission technique and then was returned to the original release media. The concentration of DOX was determined by measurement of fluorescence emission intensity at 550 nm using a standard intensity *vs* concentration curve constructed for DOX in the corresponding release buffer. By presenting the vesicles to very low pH (the solution of HCl, pH = 3.0), a nearly 100% release of DOX from DOX-loaded vesicles could be obtained.

UV−Vis Absorption and Fluorescence Emission Spectra. The UV-Vis absorption spectra were measured on a Perkin Elmer Lambda 35 UV-Vis spectrometer. The fluorescence emission spectra were recorded on a Perkin-Elmer LS55 fluorescence spectrometer.

TEM and DLS Experiments. TEM images were recorded on a JEM-2100 instrument. The sample for TEM measurements was prepared by dropping the solution onto a carbon-coated copper grid. DLS measurements were performed under a Brookhaven BI-9000AT system (Brookhaven Instruments Corporation, USA) equipped with a 200 mW laser light and operating at λ = 532 nm.

ζ-Potential Measurement. ζ-potential measurements were performed at 25 ^{o}C on a Zeta sizer-Nano Z (Malvern Instruments Ltd., Worcestershire, U.K.) using the Smoluchowski model for the calculation of the ζ-potential from the measured electrophoretic mobility.

Cell Culture. A549 cancer cells (a lung adenocarcinoma cell line) and NIH3T3 normal cells (a mouse embryonic fibroblast cell line) were cultivated, respectively, in Dulbecco's modified Eagle's medium (DMEM) supplied with 10% fetal bovine serum

(FBS) and antibiotics (50 U mL^{-1} penicillin and 50U mL^{-1} streptomycin) at 37 ^{o}C in a humidified atmosphere containing 5% CO_2.

Cytotoxicity Assay. The relative cytotoxicities of **G**, DOX, vesicles and DOX-loaded vesicles against NIH3T3 cells and A549 cells were evaluated *in vitro* by MTT assay, respectively. Briefly, the cells were seeded in 96-well plates at a density of 5000 cells per well in 200 μL DMEM, and cultured under 5% CO_2 at 37 ^{o}C for 24 h. **G** and DOX were first dissolved in DMSO to give 1 mM stock solutions which were further diluted with the culture medium, while the freshly prepared solutions of vesicles and DOX-loaded vesicles were directly diluted with the culture medium for cytotoxicity studies. The cells, after rinsed with phosphate buffered saline (PBS), were incubated with 200 μL of the above diluted solutions under 5% CO_2 at 37 ^{o}C for 24 h. Then the medium containing drug solutions was removed and 100 μL fresh medium was added. For dark cytotoxicity, the cells were incubated for another 24 h. For light cytotoxicity, the cells were exposed to LED light (λ = 690 nm) at a dose of 1.5 J cm^{-2} and then incubated for 24 h. At the end of each incubation, 20 μL of MTT solution was added into each well and the cells were incubated for 4 h. After that, the medium containing MTT was removed and DMSO (150 μL) was added to each well to dissolve the formazan crystals. Finally, the plates were shaken for 10 min, and the absorbance of formazan product was measured at 490 nm by a microplate reader (BioTek ELx808). Untreated cells in medium were used as the blank control. All experiments were carried out with three replicates. The cytotoxicity was expressed as the percentage of the cell viability relative to the blank control.

Cellular Uptake and Intracellular Localization. The cellular uptake and intracellular localization of **WP5⊃G** vesicles, DOX-loaded vesicles, and **G** were examined in A549 cancer cells. Briefly, the cells were plated onto glass-bottomed Petri dishes in 2 mL of complete culture medium for 24 h before treatment. Then cells were treated with **G** (10 μM) and **WP5⊃G** vesicles or DOX-loaded vesicles (equivalent to 10 μM **G**) at 37 ^{o}C for 5 h. After washed and replenished with fresh medium, Lyso-Tracker Red (Molecular Probes, USA) was directly added to the medium at a final concentration of 1 μM for 1 h to label lysosomes. Then the cells

were washed for three times with fresh medium and investigated by confocal laser scanning microscopy (Zeiss LSM 710). The fluorescence characteristics of **WP5⊃G** vesicles, DOX-loaded vesicles, and **G** were used to directly monitor the localization of these drugs without utilizing additional dye.

2. Synthesis of G and G_M

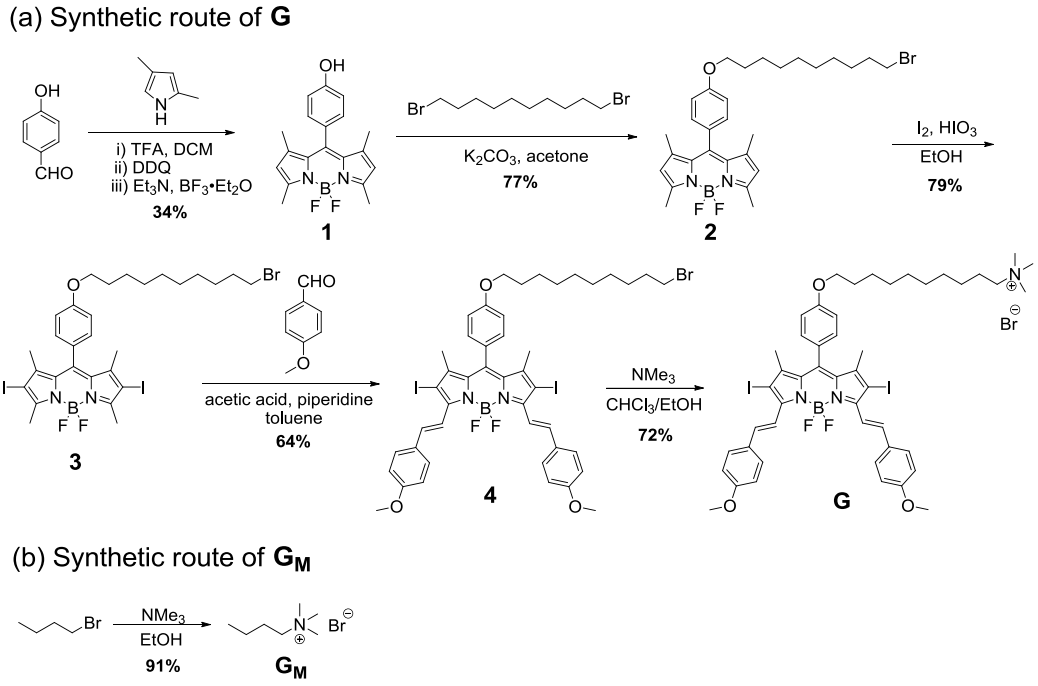

Scheme S1 Synthetic route of guests **G** and $\mathbf{G_M}$.

Compounds **1**,[S1] **2**,[S2] and desalted DOX[S3] were prepared according to previous literatures, and other synthetic procedures were described as follows:

Compound 3[S4]

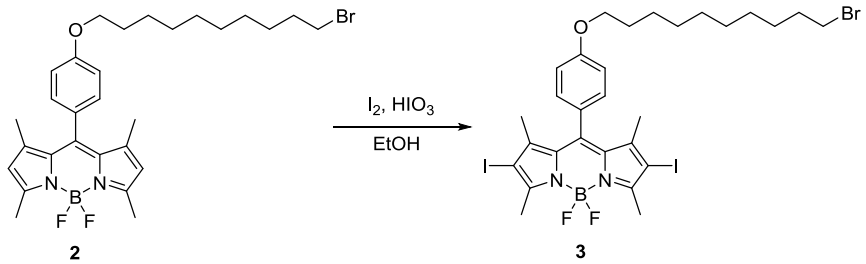

Compound **2** (0.64 g, 1.14 mmol) and iodine (0.67 g, 2.62 mmol) were added to a solution of ethanol (30 mL), and then iodic acid (0.46 g, 2.62 mmol) dissolved in 3 mL of water was added to the solution. The reaction mixture was stirred at room

temperature. When all the starting materials have been consumed, saturated $Na_2S_2O_3$ solution in water (20 mL) was added and the product was extracted into CH_2Cl_2 (3 × 30 mL). The combined organic phase was dried over anhydrous Na_2SO_4, concentrated under reduced pressure and purified by column chromatograph (silica gel, CH_2Cl_2/hexane=1/3, v/v) to give compound **3** as a red solid (0.69 g, 79%). M.p. 242–243 °C. ^{1}H NMR (300 MHz, $CDCl_3$, 298 K): δ (ppm) 7.12 (d, J = 8.7 Hz, 2H, Ar*H*), 7.02 (d, J = 8.7 Hz, 2H, Ar*H*), 4.02 (t, J = 6.6 Hz, 2H, CH_2), 3.42 (t, J = 6.6 Hz, 2H, CH_2), 2.64 (s, 6H, CH_3), 1.91–1.79 (m, 4H, CH_2), 1.55–1.25 (m, 18H, CH_2 and CH_3). ^{13}C NMR (75 MHz, $CDCl_3$, 298 K): δ (ppm) 160.3, 156.6, 145.5, 141.9, 131.88, 129.2, 126.6, 115.5, 85.7, 68.4, 34.2, 32.9, 29.6, 29.5, 29.3, 28.9, 28.3, 26.2, 17.3, 16.1. ESI-MS: *m*/*z* 848.4 $[M + K]^+$ (100%). HR-ESI-MS: calcd for $C_{29}H_{36}BBrF_2I_2N_2NaO$ $[M + Na]^+$, 835.0033, found 835.0038.

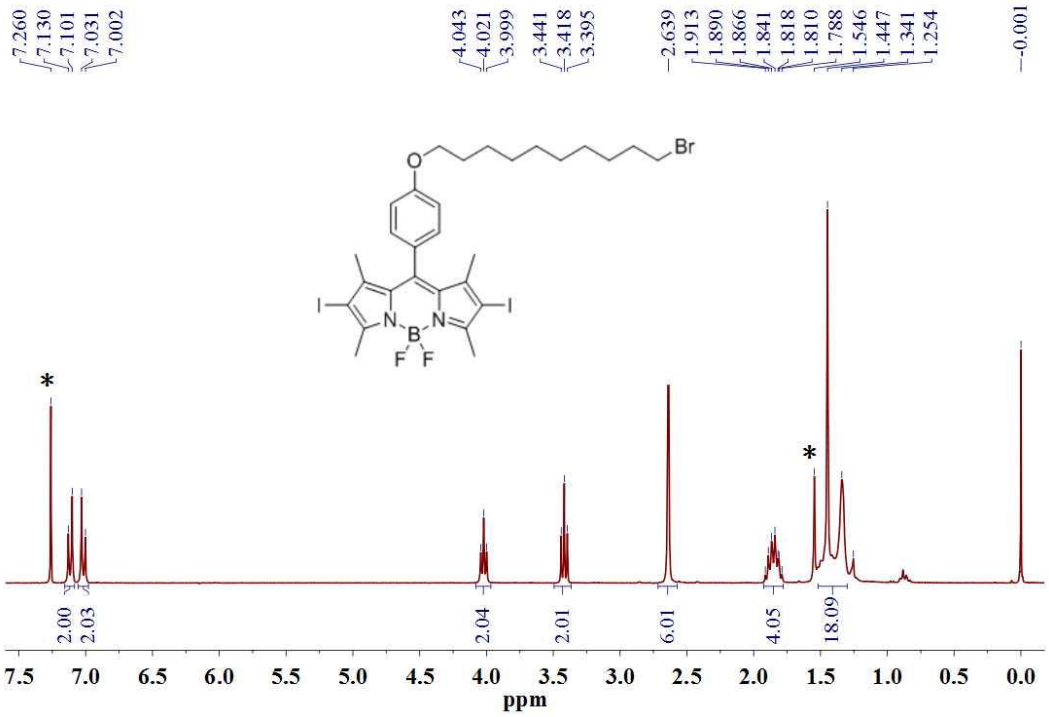

Fig. S1 ^{1}H NMR spectrum (300 MHz, $CDCl_3$, 298 K) of compound **3** (solvent peaks are marked with asterisks).

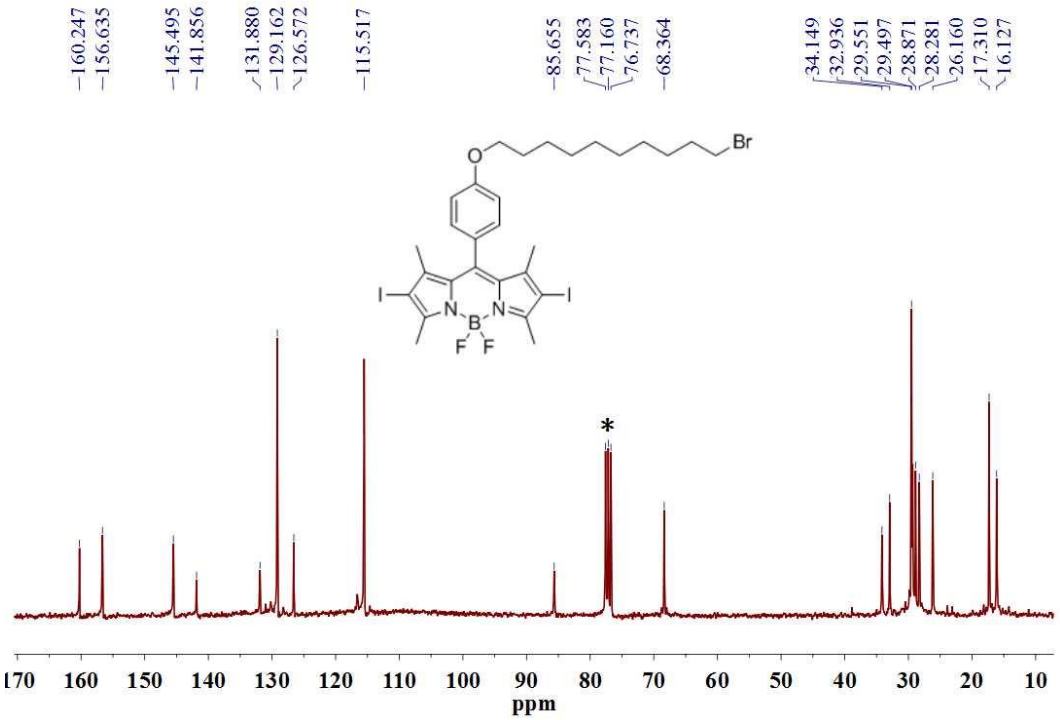

Fig. S2 ^{13}C NMR spectrum (75 MHz, $CDCl_3$, 298 K) of compound **3** (solvent peaks are marked with asterisks).

Compound 4[S5]

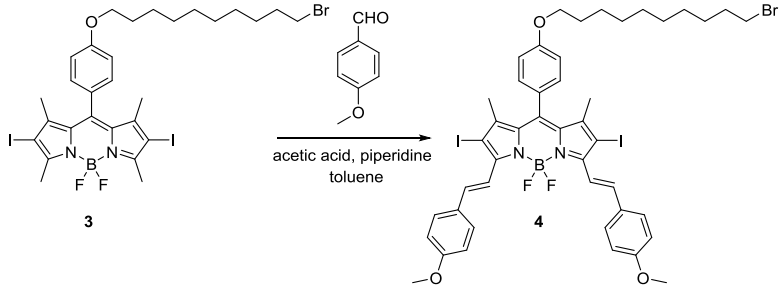

Compound **3** (87 mg, 0.11 mmol) and 4-methoxybenzaldehyde (60 mg, 0.44 mmol) were dissolved in toluene (10 mL). Glacial acetic acid (0.2 mL, 3.84 mmol) and piperidine (0.3 mL, 2.67 mmol) were added. The resulting mixture was refluxed using Dean-Stark apparatus for 20 h. Then, the solvent was evaporated under reduced pressure, and the residual was diluted with H_2O (20 mL) and extracted by CH_2Cl_2 (3 × 30 mL). The combined organic extracts were dried over anhydrous Na_2SO_4 and concentrated under reduced pressure. The crude product was purified by column chromatography (silica gel, CH_2Cl_2/hexane=1/1, v/v) to give compound **4** as a green solid (70 mg, 64%). M.p. > 300 ^{o}C. ^{1}H NMR (300 MHz, $CDCl_3$, 298 K): δ (ppm) 8.12 (br s, 2H, C=C*H*), 7.62–7.56 (m, 6H, C=C*H* and Ar*H*), 7.16 (d, J = 8.7 Hz, 2H, Ar*H*),

7.03 (d, *J* = 8.7 Hz, 2H, Ar*H*), 6.95 (d, *J* = 8.7 Hz, 4H, Ar*H*), 4.04 (t, *J* = 6.6 Hz, 2H, CH_2), 3.87 (s, 6H, CH_3), 3.42 (t, *J* = 6.6 Hz, 2H, CH_2), 1.92–1.80 (m, 4H, CH_2), 1.51–1.35 (m, 18H, CH_2 and CH_3). ^{13}C NMR (75 MHz, $CDCl_3$, 298 K): δ (ppm) 160.9, 160.2, 150.5, 145.9, 139.2, 133.4, 129.8, 129.4, 127.2, 116.9, 115.5, 114.5, 82.7, 68.4, 55.6, 34.2, 32.9, 29.5, 29.4, 28.9, 28.3, 26.2, 17.9. ESI-MS: *m*/*z* 1046.8 $[M + H]^+$ (100%). HR-ESI-MS: calcd for $C_{45}H_{48}BBrF_2I_2N_2NaO_3$ $[M + Na]^+$ 1069.0891, found 1069.0906.

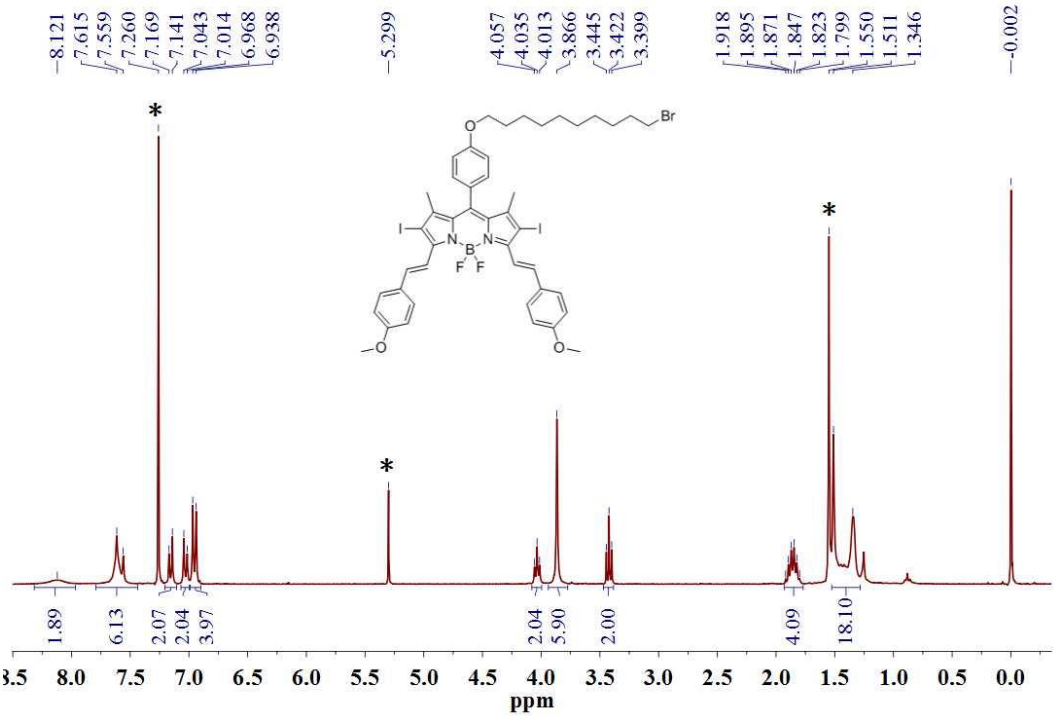

Fig. S3 ^{1}H NMR spectrum (300 MHz, $CDCl_3$, 298 K) of compound **4** (solvent peaks are marked with asterisks).

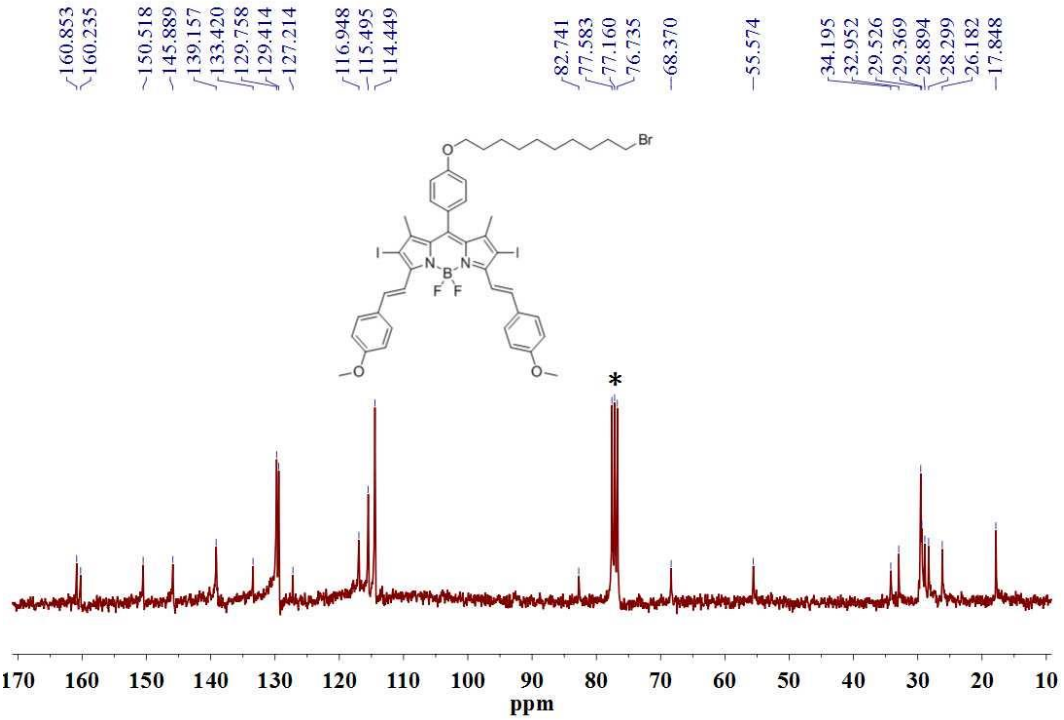

Fig. S4 ^{13}C NMR spectrum (75 MHz, $CDCl_3$, 298 K) of compound **4** (solvent peaks are marked with asterisks).

Compound G[S6]

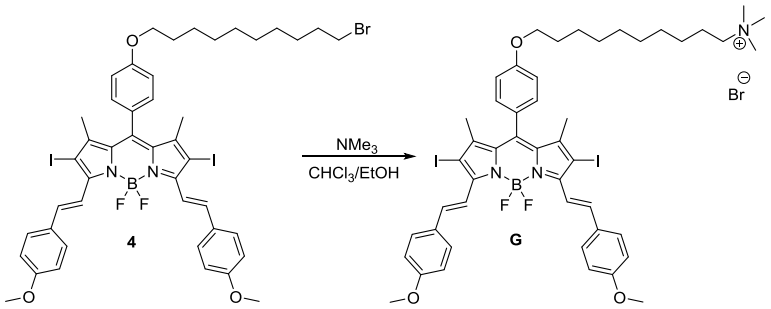

Compound **4** (0.26 g, 0.25 mmol) and trimethylamine (33% in ethanol, 0.15 g, 2.50 mmol) were added to a mixed solvents of $CHCl_3$ (15 mL) and ethanol (15 mL). The resulting solution was refluxed for 24 h in a sealed flask. Then, the mixture was concentrated under reduced pressure and purified by column chromatography (neutral alumina, CH_2Cl_2/methanol=10/1, v/v) to give compound **G** as a green solid (0.20 g, 72%). M.p. > 300 ^{o}C. ^{1}H NMR (300 MHz, $CDCl_3$, 298 K): δ (ppm) 8.16 (s, 1H, C=C*H*), 8.10 (s, 1H, C=C*H*), 7.63–7.56 (m, 6H, C=C*H* and Ar*H*), 7.15 (d, *J* = 8.4 Hz, 2H, Ar*H*), 7.03 (d, *J* = 8.4 Hz, 2H, Ar*H*), 6.95 (d, *J* = 8.4 Hz, 4H, Ar*H*), 4.03 (t, *J* = 6.3 Hz, 2H, CH_2), 3.86 (s, 6H, CH_3), 3.55 (br t, *J* = 8.4 Hz, 2H, CH_2), 3.43 (s, 9H,

CH_3), 1.84–1.79 (m, 4H, CH_2), 1.51 (s, 6H, CH_3), 1.45–1.35 (m, 12H, CH_2). ^{13}C NMR (100 MHz, DMSO-d_6, 298 K): δ (ppm) 160.7, 159.6, 149.7, 145.5, 138.6, 132.9, 129.6, 128.9, 128.6, 126.1, 116.1, 115.4, 114.8, 84.3, 67.7, 65.3, 55.4, 52.1, 28.9, 28.8, 28.6, 28.5, 25.8, 25.5, 22.0, 17.2. ESI-MS: *m*/*z* 1026.05 $[M - Br]^+$ (100%). HR-ESI-MS (ESI): calcd for $C_{48}H_{57}BF_2I_2N_3O_3$ $[M - Br]^+$ 1026.2545, found 1026.2555.

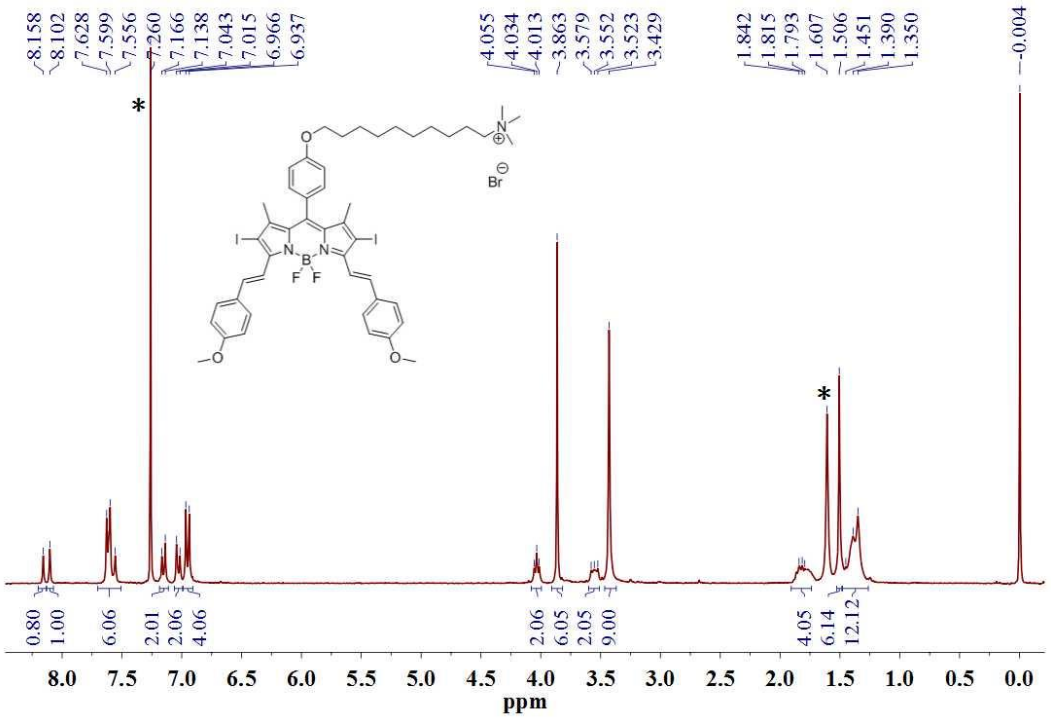

Fig. S5 ^{1}H NMR spectrum (300 MHz, $CDCl_3$, 298 K) of compound **G** (solvent peaks are marked with asterisks).

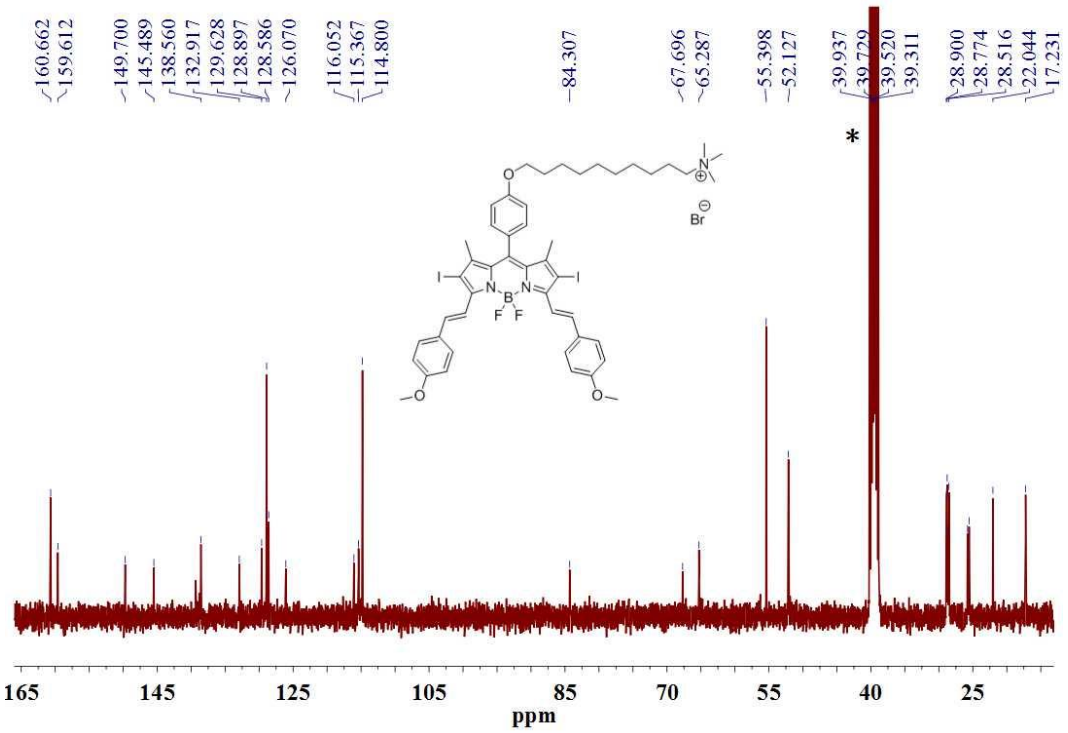

Fig. S6 ^{13}C NMR spectrum (100 MHz, DMSO-d_6, 298 K) of compound **G** (solvent peaks are marked with asterisks).

Compound $\mathbf{G_M}$[S6]

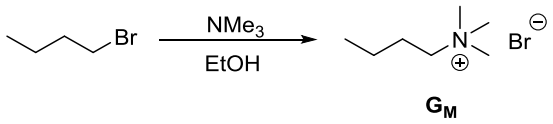

$\mathbf{G_M}$

1-bromobutane (0.50 g, 3.65 mmol) and trimethylamine (33% in ethanol, 2.15 g, 36.50 mmol) were added to ethanol (10 mL). The resulting solution was refluxed for 24 h in a sealed flask. Then, the mixture was concentrated under reduced pressure to give compound $\mathbf{G_M}$ as a colorless oil (0.65 g, 91%). ^{1}H NMR (300 MHz, $CDCl_3$, 298 K): δ (ppm) 3.61 (br t, J = 8.4 Hz, 2H, CH_2), 3.46 (s, 9H, CH_3), 1.79–1.68 (m, 2H, CH_2), 1.49–1.37 (m, 2H, CH_2), 0.99 (t, J = 7.2 Hz, 3H, CH_3). ^{13}C NMR (75 MHz, $CDCl_3$, 298 K): δ (ppm) 66.7, 53.5, 25.1, 19.6, 13.8. ESI-MS: m/z 116.1 $[M - Br]^+$ (100%). HR-ESI-MS (ESI): calcd for $C_7H_{18}N$ $[M - Br]^+$ 116.1434, found 116.1434.

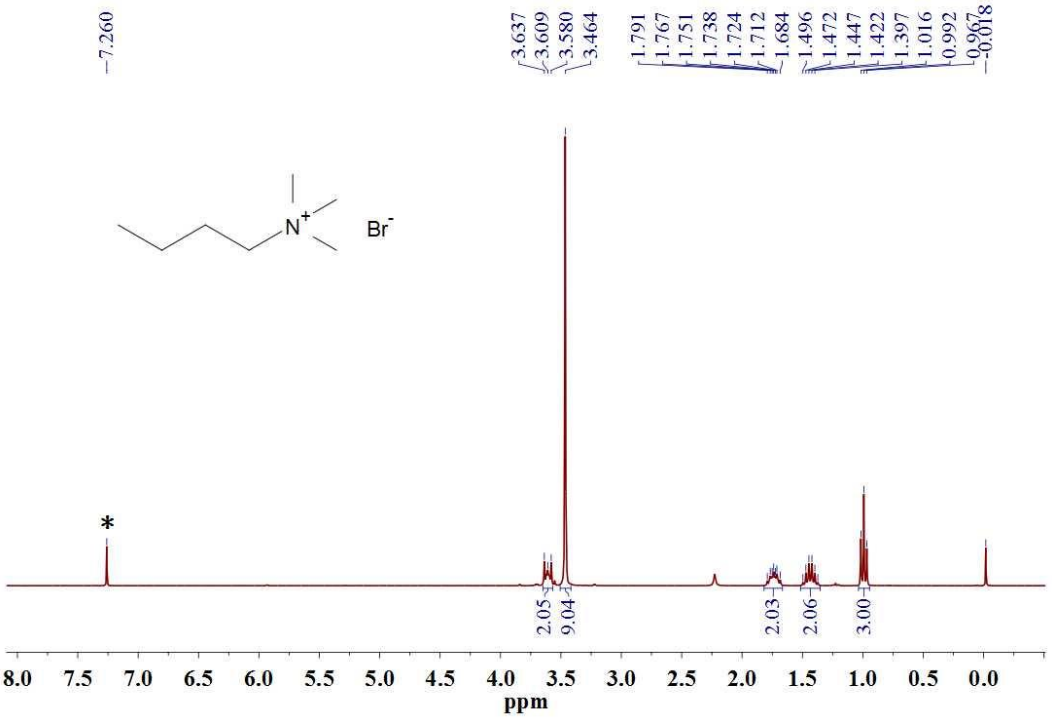

Fig. S7 ^{1}H NMR spectrum (300 MHz, $CDCl_3$, 298 K) of compound $\mathbf{G_M}$ (solvent peaks are marked with asterisks).

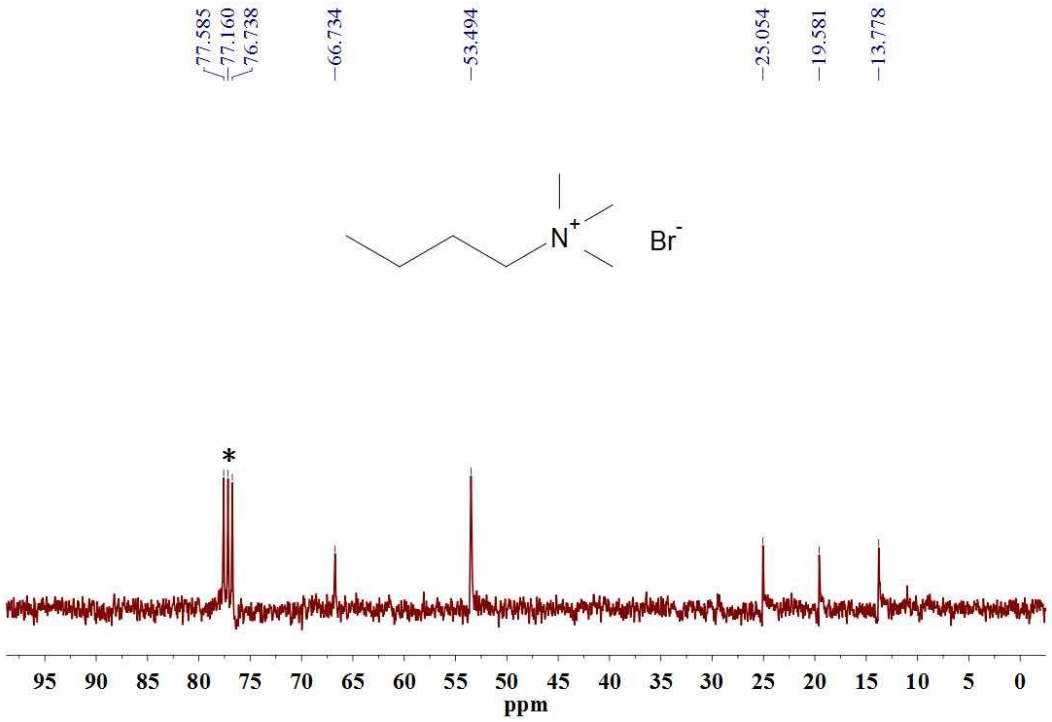

Fig. S8 ^{13}C NMR spectrum (75 MHz, $CDCl_3$, 298 K) of compound $\mathbf{G_M}$ (solvent peaks are marked with asterisks).

3. 2D ROESY spectrum of WP5⊃G_M

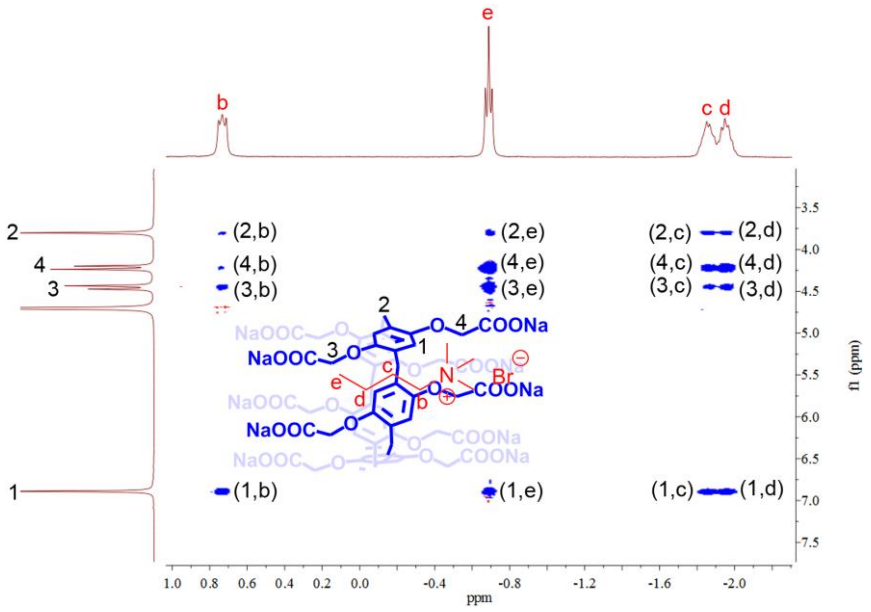

Fig. S9 Partial 2D ROESY spectrum (400 MHz, D2O, 298 K) of complex **WP5⊃G_M** ([**WP5**] = [G_M] = 40 mM).

4. Job plot for WP5⊃G_M

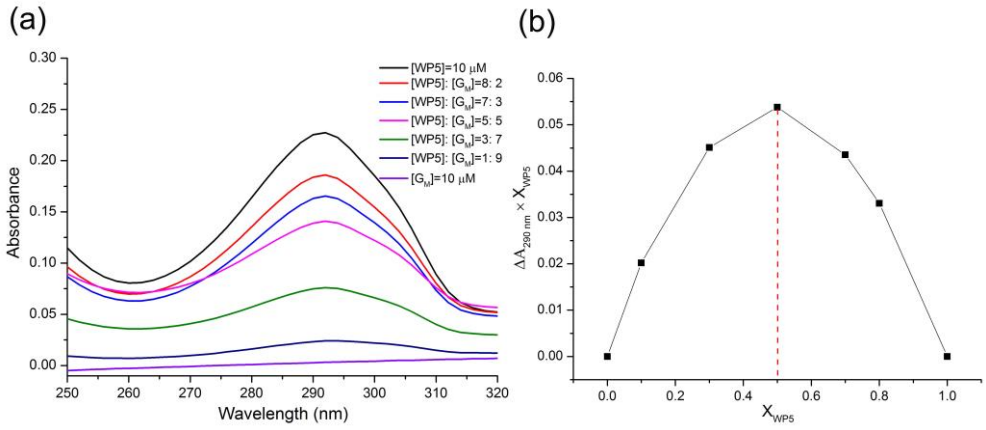

Fig. S10 (a) UV-Vis absorption spectra of complex **WP5⊃G_M** with different molar ratios in water while [**WP5**] + [G_M] = 10 μM. (b) Job plot of complex **WP5⊃G_M** showing a 1:1 stoichiometry between **WP5** and G_M by plotting the absorbance difference at 290 nm (a characteristic absorption peak of **WP5**) against the mole fraction of **WP5**.

5. Determination of the association constant for WP5⊃G_M

To determine the association constant for the complexation between **WP5** and G_M, ^{1}H NMR titration experiments were carried out in D_2O, which had a constant concentration of G_M (2 mM) and varying concentrations of **WP5**. By a non-linear curve-fitting method, the association constant (K_a) of **WP5⊃G_M** was estimated to be

$(5.46 \pm 1.27) \times 10^3\ M^{-1}$, which was approximated as the K_a value between **WP5** and **G**. The non-linear curve-fittings were based on the equation:

$$\Delta\delta = (\Delta\delta_\infty/[G]_0)\ (0.5[H]_0 + 0.5([G]_0 + 1/K_a) - (0.5([H]_0^2 + (2[H]_0(1/K_a - [G]_0)) + (1/K_a + [G]_0)^2)^{0.5})) \quad \text{(eq. S1)}$$

Where $\Delta\delta$ is the chemical shift change of Ha on $\mathbf{G_M}$ at $[H]_0$, $\Delta\delta_\infty$ is the chemical shift change of Ha when the guest is completely complexed, $[G]_0$ is the fixed initial concentration of the guest, and $[H]_0$ is the varying concentration of **WP5**.

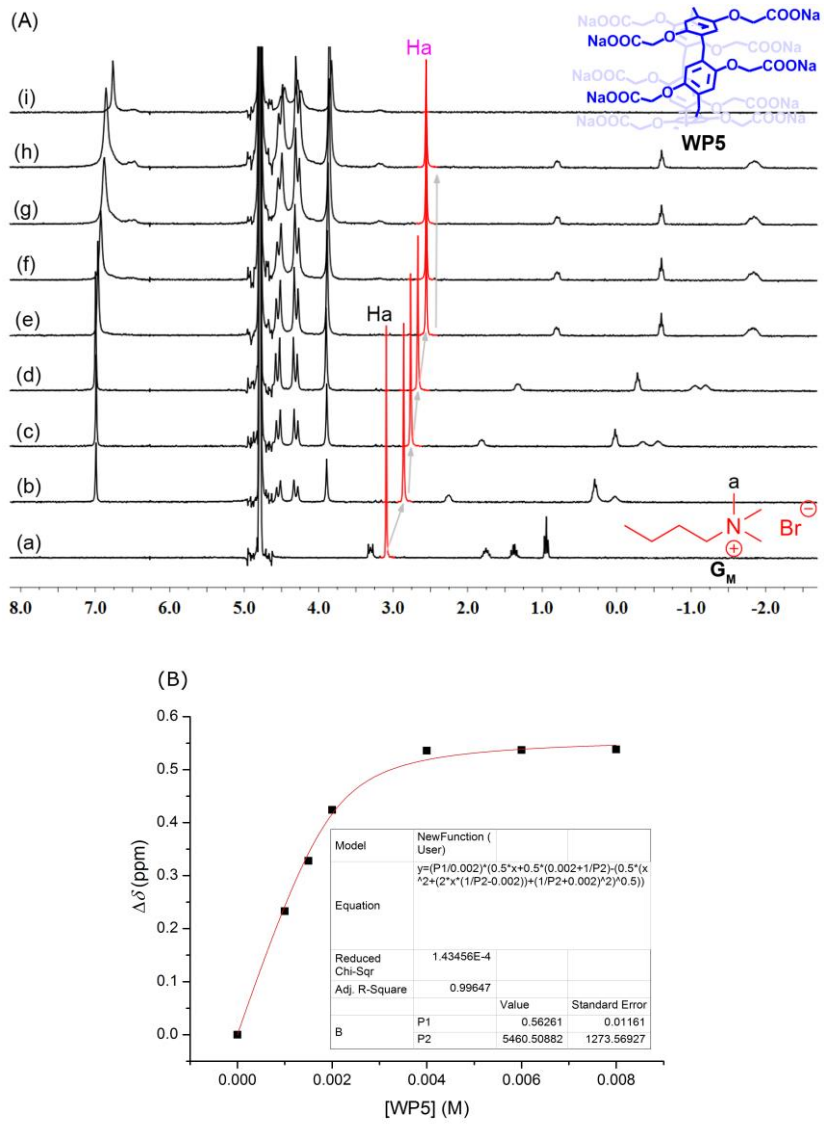

Fig. S11 (A) ^{1}H NMR spectra (300 MHz, D_2O, 298 K) of $\mathbf{G_M}$ at a constant concentration of 2.0 mM with different concentrations of **WP5** (mM): (a) 0.00, (b) 0.50, (c) 0.75, (d) 1.00, (e) 1.50, (f) 2.00, (g) 3.00, (h) 4.00, and (i) individual **WP5** (2.0 mM). (B) The chemical shift changes of Ha on $\mathbf{G_M}$ upon the addition of **WP5**. The red solid line was obtained from the non-linear curve-fitting using eq. S1. The association constant of **WP5** and $\mathbf{G_M}$ was estimated to be $(5.46 \pm 1.27) \times 10^3\ M^{-1}$.

6. The aggregation behavior of WP5⊃G in aqueous solution

The best molar ratio between **WP5** and **G** for constructing these supramolecular aggregates was investigated by UV−Vis absorption spectroscopy. As shown in Fig. S12, upon gradually increasing the amount of **WP5**, the absorbance at 750 nm underwent a sharp increase and then an inverse decrease. The rapid increase of the absorbance implied that **WP5** and **G** formed a higher-order complex with a tendency toward amphiphilic aggregation, whereas it disassembled upon further addition of **WP5**, generating a simple 1:1 supramolecular inclusion complex. Therefore, the best molar ratio of **WP5** and **G** for the formation of supramolecular aggregates was obtained in the inflection point (([**WP5**]/[**G**] = 1/8).

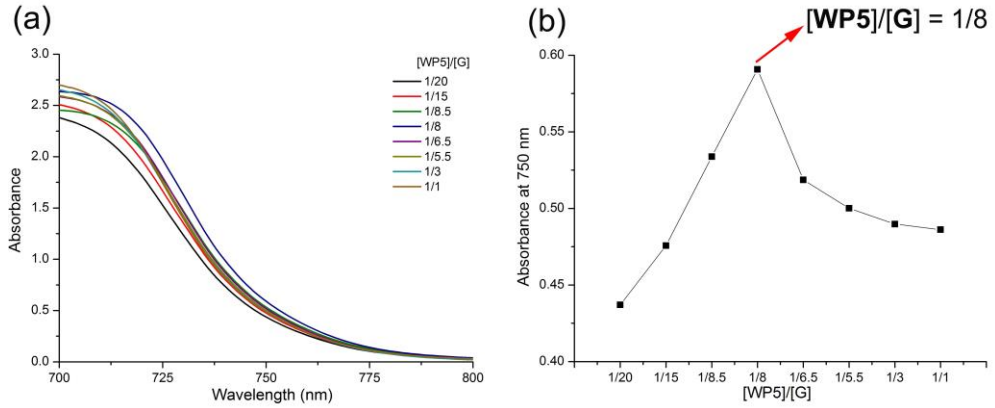

Fig. S12 (a) UV−Vis absorption of a mixture of **WP5** and **G** in water with constant **G** concentration (5×10^{-5} M) upon increasing the concentration of **WP5** (0.05–1.00 equiv.) at 25 °C. (b) Dependence of the relative absorption intensity at 750 nm on the **WP5** concentration with a fixed concentration of **G** (5×10^{-5} M) at 25 °C.

7. Dependence of fluorescence intensity on concentration of DOX

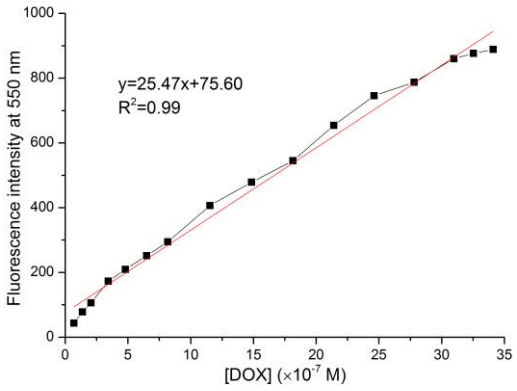

Fig. S13 Dependence of fluorescence emission intensity of DOX at 550 nm on the DOX concentration in water at 25 °C.

8. pH-Responsive DOX release behavior

The release behavior of DOX from the DOX-loaded **WP5⊃G** vesicles could be controlled by changing the solution pH. The release profiles of DOX under different pH conditions were presented in Fig. S14, from which a good pH-dependent DOX release behavior could be clearly observed. The cumulative release of DOX was only about 12% within 24 h under the physiological condition (pH 7.4), implying good stability of these **WP5⊃G** vesicles. However, by adjusting the solution pH to acidity, DOX was released in abundant amounts of 53% at pH 6.0 and 86% at pH 5.1 within 24 h, respectively. In particular, obvious rapid DOX release was observed in the first 1 h under acidic conditions, which could be well explained by the pH-triggered disintegration of these vesicles leading to the rapid release of the encapsulated drugs. Considering the microenvironment of tumor cells is acidic for both intracellular and extracellular compartments due to the presence of excessive lactic acid and CO_2 as metabolites, so the rapid release of DOX from **WP5⊃G** vesicles can be triggered by the acidic microenvironment in tumor tissues, which is extremely significant for specific targeted therapy, making such supramolecular vesicles potential and promising DDS candidates for cancer therapy.

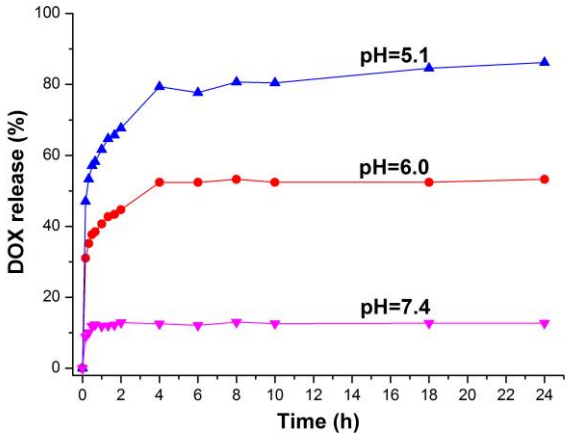

Fig. S14 pH-Responsive DOX release profiles of the DOX-loaded **WP5⊃G** vesicles in the release media of different pH values.

9. The cytotoxicities of G and WP5⊃G vesicles against NIH3T3 cells

Since the biocompatibility of DDSs is a significant index for biomedical applications and **WP5** has been proved to be biocompatible in aqueous media, the *in vitro* cytotoxicities of **G** and **WP5⊃G** vesicles were first investigated against NIH3T3 normal cells (a mouse embryonic fibroblast cell line) via MTT assay. Fig. S15 shows the dose-dependent relative cell viability profiles of **G** and **WP5⊃G** vesicles at concentrations varying from 0.005 to 1 μM for **G** and 0.50 to 20 μM for **WP5⊃G** vesicles. Obviously, the cell viability remains above 85% even when the concentration of **G** or **WP5⊃G** vesicles increases to maximum measured value, implying the good biocompatibility of this supramolecular nanocarrier as DDSs

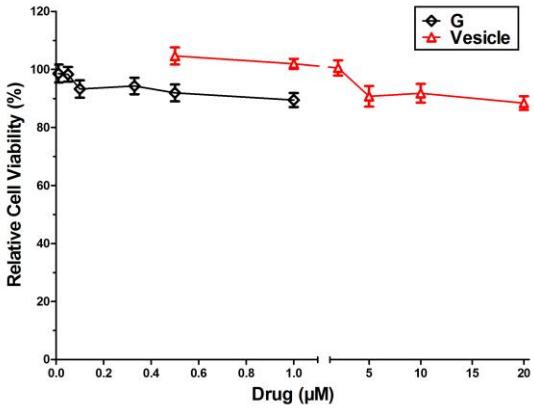

Fig. S15 The cytotoxicities of **G** and **WP5⊃G** vesicles against NIH3T3 normal cells, respectively. Data were treated as mean values ± S.E.M. of three independent experiments, each performed in quadruplicate.

10. UV−Vis absorption spectrum of G in aqueous solution

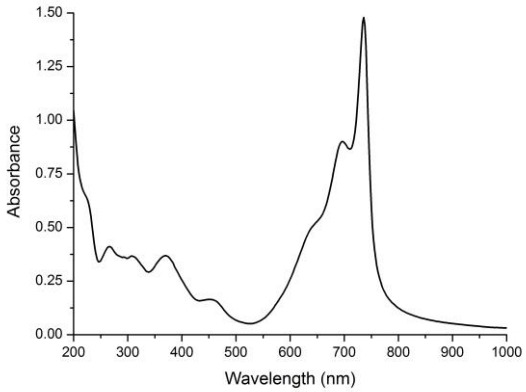

Fig. S16 UV−Vis absorption spectrum of **G** in water ([**G**] = 5 × 10^{-5} M).

11. Table of IC_{50} values against A549 cancer cells

Table S1 IC_{50} values of **G**, DOX, vesicles, and DOX-loaded vesicles against A549 cancer cells upon irradiation and in the dark, respectively.

Drug	IC_{50}/μM	
	irradiation	dark
G	0.08	-
DOX	0.20	0.22
vesicles[a]	0.70	-
DOX-loaded vesicles[a]	1.40	5.50

[a] The IC_{50} values were calculated based on the **G** concentration.

12. Singlet Oxygen Detection in Aqueous Solution

The generation of singlet oxygen photosensitized by BODIPY guest **G** or **WP5⊃G** vesicles in aqueous media was investigated according to Kraljic's method.[S7] Solutions of *p*-nitrosodimethylaniline (RNO, 30 μM), imidazole (0.5 mM) in PBS (10 mM, pH = 7.4) was added **G** (10 μM) or vesicular solution (10 μM), which was then irradiated (λ = 690 nm, 1.5 J cm^{-2}) for different periods of time, and the absorbance reduction of RNO at 440 nm was plotted against irradiation time. As shown in Fig. S17, the control (without addition of **G** or vesicular solution) almost remains unchanged absorbance while the absorbance decreases remarkably with the addition of **G** or vesicular solution upon irradiation, which confirms that singlet oxygen is indeed induced by BODIPY guest **G** or vesicles formed by BODIPY guest and **WP5**.

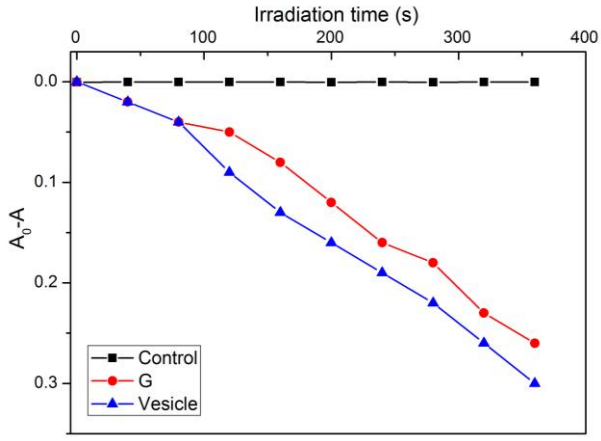

Fig. S17 The photooxidation of RNO upon irradiation showing the generation of singlet oxygen photosensitized by **G** or vesicles.

13. References

S1. Q. Wang, H. Lu, L. Gai, W. Chen, G. Lai and Z. Li, *Dyes Pigments*, 2012, **94**, 183.

S2. T. Toyota, K. Takakura, Y. Kageyama, K. Kurihara, N. Maru, K. Ohnuma, K. Kaneko and T. Sugawara, *Langmuir*, 2008, **24**, 3037.

S3. Y. Cao, X.-Y. Hu, Y. Li, X. Zou, S. Xiong, C. Lin, Y.-Z. Shen and L. Wang, *J. Am. Chem. Soc.*, 2014, **136**, 10762.

S4. S. Banfi, G. Nasini, S. Zaza and E. Caruso, *Tetrahedron*, 2013, **69**, 4845.

S5. W.-J. Shi, P.-C. Lo, A. Singh, I. Ledoux-Rak and D. K. P. Ng, *Tetrahedron*, 2012, **68**, 8712.

S6. T. Toyota, H. Tsuha, K. Yamada, K. Takakura, K. Yasuda and T. Sugawara, *Langmuir*, 2006, **22**, 1976.

S7. I. Kraljić and S. E. Mohsni, *Photochem. Photobiol.*, 1978, **28**, 577.